AD 687738

MAY 28 1969

DREXEL INSTITUTE OF TECHNOLOGY

Reproduced by the
CLEARINGHOUSE
for Federal Scientific & Technical
Information Springfield Va. 22151

38

DISCLAIMER NOTICE

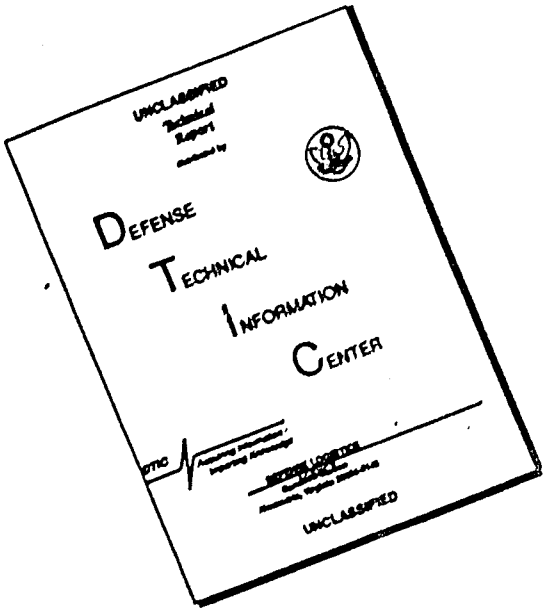

THIS DOCUMENT IS BEST QUALITY AVAILABLE. THE COPY FURNISHED TO DTIC CONTAINED A SIGNIFICANT NUMBER OF PAGES WHICH DO NOT REPRODUCE LEGIBLY.

SPHEROIDIZATION OF BINARY IRON-CARBON ALLOYS OVER A RANGE OF TEMPERATURES

K. M. Vedula and R. W. Heckel

Technical Report No. 1

Office of Naval Research
Contract N00014-67-A-0406-002
NR 031-714/2-6-67

April 1969

Reproduction in whole or in part is permitted
for any purpose of the United States Government

Distribution of this document is unlimited

Drexel Institute of Technology
Department of Metallurgical Engineering
Philadelphia, Pa. 19104

MAY 28 1969

SPHEROIDIZATION OF BINARY IRON-CARBON ALLOYS OVER A RANGE OF TEMPERATURES

K. M. Vedula* and R. W. Heckel**

Abstract

The spheroidization of cementite in binary iron-carbon alloys (0.24, 0.42, and 0.79 weight percent carbon) was investigated over a range of temperatures (594, 649, and 704°C) for times up to about 10^6 seconds. Quantitative metallography techniques were used to obtain the following microstructural data on the cementite particles: shape, size distribution, mean size, number of particles per unit volume, and growth (and shrinkage) rates of various sizes in the size distribution. The variations of these microstructural parameters were analyzed in terms of existing models for the spheroidization process.

The Lifshitz-Wagner analysis is shown to have limited applicability to the spheroidization of cementite in binary steels, since the required steady-state size distribution is not attained in times less than about 10^6 seconds. An analysis similar to that of Lifshitz and Wagner, but requiring no specification of the shape of the size distribution, is shown to apply and indicates that the observed spheroidization was diffusion-controlled. The effective diffusion coefficient was between the values for the diffusion of carbon and iron in ferrite and approximated the coupled diffusion coefficients developed by Oriani and Li, Blakely, and Feingold.

*Graduate Student, Materials Engineering, Drexel Institute of Technology, Philadelphia, Pa.

**Professor of Metallurgical Engineering, Drexel Institute of Technology, Philadelphia, Pa.

I. INTRODUCTION

The spheroidization of cementite in the iron-carbon system has been considered previously in several theoretical and experimental investigations. The Lifshitz-Wagner (1-4) theory predicts that, when the steady-state size distribution of cementite particles is attained, the kinetics may be described by Equation 1 or 2:

(i) for diffusion-controlled growth:

$$\bar{R}^3 - \bar{R}_0'^3 = \frac{8 \sigma D C_0 V_m^2 (t - t_0')}{9 \nu R T} \qquad (1)$$

(ii) for interface-controlled growth:

$$\bar{R}^2 - \bar{R}_0'^2 = \frac{64 \sigma k C_0 V_m^2 (t - t_0')}{81 \nu R T} \qquad (2)$$

where:

$\bar{R}$ is the mean particle radius at any time t,

$\bar{R}_0'$ is the mean particle radius at any time, t_0', when steady-state growth begins,

σ is the surface free energy of the interface (assumed isotropic),

D is the diffusion coefficient,

C_0 is the equilibrium solubility under conditions where all particles have a radius of curvature of infinity,

V_m is the molar volume of cementite based on the formula Fe_3C,

R is the gas constant,

T is the absolute temperature,

k is the reaction constant, and

ν is the stoichiometric factor (weight fraction of solute in particles).

Bannyh, Modin and Modin (5) were among the first to obtain quantitative experimental data for the spheroidization of cementite in steel. They de-

termined the mean particle size as a function of spheroidizing time for a eutectoid steel of commercial purity. $\bar{R}$ was found to be proportional to $t^{1/3}$ at 700°C, in agreement with the Lifshitz-Wagner (1-4) theory for diffusion-controlled growth. At lower temperatures agreement was poor.

Heckel (6) has presented mathematical models, adapted from the Lifshitz-Wagner theory, for five rate-controlling mechanisms. These models have the advantages of being able to treat any input size distribution and, therefore, require no assumption of a steady-state distribution. Two of these models are given by Equations 3 and 4:

(i) for diffusion-controlled growth (minimum rate):

$$\frac{dx_i}{dt} = \frac{D}{8\nu\rho\left(\frac{3}{4\pi N_T}\right)^{1/3}}\left[\left(\frac{1}{x_i^2}\sum_{j=1}^{i-1} x_j^2\,\Delta C_{ij}\right) + \left(\sum_{j=i+1}^{n}\Delta C_{ij}\right)\right] \qquad (3)$$

(ii) for interface-controlled growth, limited by the reaction of the deposition (growing) interfaces (reaction rate proportional to the solute thermodynamic activity gradient across the interface):

$$\frac{dx_i}{dt} = -\frac{K_1}{\nu\rho}\left[\left(\frac{1}{n-1}\sum_{j=1}^{i-1}\Delta C_{ij}\right) + \left(\frac{1}{x_i^2}\sum_{j=i+1}^{n}\Delta C_{ij}\frac{x_j^2}{(j-1)}\right)\right] \qquad (4)$$

where:

x_i is the radius of the particle whose growth rate is being calculated,

x_j is the radius of any of the jth neighbors surrounding the ith,

D is the diffusion coefficient,

ρ is the density of the second phase,

N_T is the number of second-phase particles per unit volume,

K_1 is the reaction rate constant, and

ΔC_{ij} is the difference between the solubilities of the solute in the matrix adjacent to the ith and j^{th} particles. ΔC_{ij} may be

calculated from Equation 5:

$$\Delta C_{ij} = C_0 \left(\exp \frac{2\sigma V_m}{RTx_i} - \exp \frac{2\sigma V_m}{RTx_j} \right) \qquad (5)$$

Heckel and DeGregorio (7) used these models for their study of a binary Fe - 0.75C steel spheroidized at 704°C for various times. The diffusion-controlled model (Equation 3 using the diffusion coefficient for carbon in ferrite [$D_C = 6.75 \times 10^{-7}$ cm^2/sec]), gave spheroidization rates that differed from their experimental data by one to two orders of magnitude. Since the rates predicted by the interface-controlled growth model represented by Equation 4 (with $K_1 = 2 \times 10^{-5}$ cm/sec) provided the best fit to their data, they concluded that the process was controlled by the deposition of solute at growing interfaces (the rate being proportional to the thermodynamic activity gradient across the interface).

It has been proposed that the appropriate diffusion coefficient for spheroidization is not that of the solute in the matrix, but is a coupled diffusion coefficient. Oriani (8-9) has considered this problem from a volume transfer standpoint where the driving forces and resistive drags of both components in the binary system are coupled. He formulated the following expression for the effective diffusion coefficient for the spheroidization process:

$$D^0 = \frac{2 V_C D_C D_{Fe}}{V_C D_{Fe} + n_C V_C^2 D_{Fe} + V_{Fe} D_C - V_{Fe}^2 n_{Fe} D_C} \qquad (6)$$

where:

n_{Fe}, n_C are the concentrations in ferrite of iron and carbon, respectively,

V_{Fe} is the atomic volume of iron in ferrite,

V_C is the difference between the volume of one molecule of Fe_3C and

the volume of three atoms of iron in ferrite, and

D_{Fe}, D_C are the diffusion coefficients of iron and carbon in ferrite, respectively.

Li, Blakely, and Feingold (10) have developed a coupled diffusion analysis which considers composition constraints as well as volume constraints. Their expression for the effective diffusion coefficient for spheroidization of cementite in ferrite matrix is:

$$D^{LBF} = \frac{n_{Fe} D_{Fe} D_C V_{Fe}}{n_{Fe} D_{Fe} V_{Fe}^2 + n_C D_C V_C^2} \left(V_{Fe} + \frac{n_C}{n_{Fe}} V_C \right) \qquad (7)$$

Comparison of the values provided by Equations 6 and 7 for coupled diffusion at 700°C shows that $D^0 = 6.4 \times 10^{-10}$ cm^2/sec and $D^{LBF} = 9.2 \times 10^{-10}$ cm^2/sec, both of which are intermediate between the diffusion coefficients of carbon and iron in ferrite (8.7×10^{-7} cm^2/sec (11) and 6.3×10^{-14} cm^2/sec (12), respectively.

Airey, Hughes, and Mehl (13) investigated 0.15C steels with various alloying elements. Their data were plotted in accordance with the Lifshitz-Wagner (1-4) analysis assuming diffusion control, and reasonable agreement was found. Their calculated σ values, using D^{LBF} and Equation 1, reached unlikely high values at low spheroidization temperatures, and abnormally low values for some alloy steels.

The above mentioned studies provide a variety of experimental data, analytical models, and conclusions to the mechanism of spheroidization in steels. Many factors may have contributed to the inconsistency in conclusions. Experimentally, the purity of steels used has not always been high and data have not always been obtained over large ranges of temperature, carbon concentration and time. In the treatment of their data, investigators have

generally applied only a single method of data analysis. The present study was designed to overcome these drawbacks. Extensive data were obtained for relatively large ranges of temperature, carbon concentration and time. Pure iron-carbon steels were used and the data were analyzed in terms of Lifshitz-Wagner theory (1-4), the adaption of the Lifshitz-Wagner theory used previously by Heckel and DeGregorio (6,7), and a newly-developed method. Values of diffusion coefficients obtained from the analyses of Oriani (8,9) and Li, Blakely, and Feingold (10) have been used in the mathematical models for diffusion-controlled spheroidization along with diffusion coefficients for iron and carbon in ferrite. The results of all of these analyses have been compared to the experimental data in order to develop an understanding of the spheroidization mechanism and to resolve some of the controversy that currently exists in the literature.

II. EXPERIMENTAL PROCEDURE AND RESULTS

A. Materials

The steels used in the present investigation were obtained in the form of 1/2 inch diameter, vacuum-melted, chill-cast, laboratory ingots. Compositions of the three steels used are given in Table I. Consistency in the spheroidization data indicated that the impurity levels were low enough to consider these steels as binary Fe-C alloys.

B. Heat Treatment

The ingots were cut into slices (about 1/8 inch thick) and mounted on steel wires in preparation for austenitizing, quenching, and spheroidizing. Table II lists the heat treatments given.

C. Quantitative Metallography

Photomicrographs were taken at 1000X and enlarged to about 3000X to facilitate accurate particle measurements. Figure 1 illustrates the type of structure observed for the Fe - 0.79C steel spheroidized at 704°C for various times. Cementite particle size distributions for each specimen were obtained by using the DeHoff (14) analysis for ellipsoids of revolution of constant shape. The major and minor axes, for the best fitting ellipse, for each particle observed on the photomicrograph, were measured and grouped into size classes. Between 500 and 1500 particles were measured in the determination of each size distribution. This random plane size distribution of particles was converted to a volume size distribution using Equation 8:

$$N_j = \frac{1}{k(q)\cdot\Delta} \sum_{i=j}^{k} n_i \cdot \beta(j,i) \qquad (8)$$

where:

N_j are the number of particles in the jth size class per unit volume,

k is the number of size classes,

$k(q)$ is the shape factor, a function of $q = B_j/A_j$,

A_j, B_j are the major and minor axes of the ellipsoid of revolution, respectively,

Δ is the size class increment,

n_i are the number of particles in the ith size class per unit area, and

$\beta(j,i)$ are the Saltykov coefficients (14).

The volume fraction of cementite, V_T, and the total cementite:ferrite surface area per unit volume, S_T, may be obtained from the size distribution data using Equations 9 through 12:

$$V_T\,(\text{oblate}) = \sum_{j=1}^{k} N_j \cdot \frac{\pi}{6} (A_j)^2 (B_j) \qquad (9)$$

$$V_T\,(\text{prolate}) = \sum_{j=1}^{k} N_j \cdot \frac{\pi}{6} (A_j)(B_j)^2 \qquad (10)$$

$$S_T(\text{oblate}) = \sum_{j=1}^{k} N_j \left[\frac{\pi (A_j)^2}{2} + \frac{\pi (B_j)^2}{4\epsilon} \cdot \ln\left(\frac{1+\epsilon}{1-\epsilon}\right) \right] \qquad (11)$$

$$S_T(\text{prolate}) = \sum_{j=1}^{k} N_j \left[\frac{\pi (B_j)^2}{2} + \frac{\pi (A_j)(B_j)}{2\epsilon} \sin^{-1}\epsilon \right] \qquad (12)$$

where:

$$\epsilon = \frac{[(A_j)^2 - (B_j)^2]^{1/2}}{(A_j)}$$

The appropriate value of q and the particle shape (oblate or prolate) were determined by comparing V_T and S_T values obtained from Equations 9 through 12 to values obtained by size and shape insensitive techniques. Point counting and lever rule calculations were used to obtain V_T. The Smith and Guttman technique (15) was used to obtain S_T :

$$S_T = 2 N_L \qquad (13)$$

where N_L is the number of intercepts of cementite:ferrite interface per unit length of test line. An oblate shape with the q values given in Table III was found to give the best agreement between V_T and S_T values obtained from Equations 9 through 12 and values obtained by the size and shape insensitive techniques mentioned above. Table III shows the mean value of q to be 0.73 with no systematic variation with temperature, time and/or composition. Typical variations in cementite size distributions (obtained from the DeHoff analysis (Equation 8 and q values in Table III) as a function of spheroidizing time are shown in Figure 2 for the Fe - 0.79C steel spheroidized at 704°C.

The mean particle size for each size class, R_j , the mean overall particle size for each specimen, $\bar{R}$, and the total number of particles per unit volume, N_T , for each specimen were calculated using Equations 14 through 16:

$$R_j = \frac{2A_j + B_j}{6} \qquad \text{(oblate)} \qquad (14)$$

$$\bar{R} = \frac{\sum_{j=1}^{k} N_j R_j}{\sum_{j=1}^{k} N_j} \qquad (15)$$

$$N_T = \sum_{j=1}^{k} N_j \qquad (16)$$

Figure 3 shows the variation of N_T with spheroidizing time for all specimens. Figure 4 gives the variation of $(\bar{R}^3 - \bar{R}_0^3)$ as a function of $(t - t_0)$ where $\bar{R}_0$ and t_0 are the mean radius and spheroidizing time for the specimen spheroidized for the shortest time at each temperature.

III. DISCUSSION

A. Analysis of size distribution changes with time

Steady-state kinetics is observed, according to the Lifshitz-Wagner (1-4) theory, after a steady-state size distribution of cementite particles is attained. Equations 1 and 2 describe the steady-state growth for diffusion-controlled and interface-controlled mechanisms, respectively. Wagner (1) has given the shape of the steady-state size distribution curve to be expected for diffusion-controlled growth (Figure 5 - dashed curve).

In the present investigation, experimental size distribution curves of the type shown in Figure 2 were normalized for comparison to this steady-state size distribution by dividing each distribution into 12 equal increments on a scale of $R_j/\bar{R}$ ranging from 0 to 3.0. Histograms thus obtained were approximated by continuous curves. Figure 5 shows the normalized experimental size distribution curves for the Fe - 0.79C steel spheroidized at 704°C, compared to the predicted steady-state distribution. Although the experimental size distributions approached the steady-state size distributions with increasing spheroidizing time, steady-state was not attained in the range of time covered by the present investigation.

Ardell and Nicholson (16) investigated spheroidization of γ' in the Ni-Al system and found that the steady-state size distribution was attained

at very short times. They obtained good agreement with the Lifshitz-Warner theory for diffusion-controlled kinetics. Apparently, the Fe-C system approaches steady-state spheroidization much more slowly.

B. Analysis of $\bar{R}$ vs. t data

The variation of mean radius, $\bar{R}$, with spheroidizing time, t, was studied using Equations 1 and 2 in order to evaluate their applicability to size distributions which only approached the steady-state. $\bar{R}_o$ and t_o, values at the initial stages of observed spheroidization, were substituted in Equations 1 and 2 for the values at the onset of steady state, $\bar{R}_o'$ and t_o'. Figure 4 shows the experimentally observed behavior of $(\bar{R}^3-\bar{R}_o^3)$ vs. $(t-t_o)$ for all compositions and temperatures studied. The slopes of the lines are given in Table IV. The slopes generally increase with increasing temperature and appear to approach 1.00. Application of Equations 1 and 2 to steady-state size distributions (using $\bar{R}_o'$ and t_o') should provide a slope of 1.00 for diffusion control and 1.50 for interface-reaction control. The data of the present investigation suggest a diffusion-controlled mechanism, with the deviations of slopes below 1.00 being due to non-steady-state conditions and the arbitrary selection of values for $\bar{R}_o$ and t_o.

The data points in Figure 4 were used to obtain values corresponding to D in Equation 1, by forcing a slope of 1.00 on them and measuring the intercepts. Values of σ = 700 ergs/cm^2, V_m = 24.3 cm^3 per mole, R = 8.32 x 10^7 ergs per mole - K°, ν = 0.067 and C_o values at different temperatures from the literature (17) were used for the calculation of D from the intercept value. Table V lists the calculated values of D. The slope of log D vs. $1/T$ was not constant and may be attributed to the non-steady-state kinetics. This will be discussed in further detail later.

C. Analysis of size distribution to get dx_i/dt .

This method of analysis was basically similar to that used by Heckel and DeGregorio (7). Experimental size distribution curves were compared as a function of spheroidizing time to obtain values of dx_i/dt, the growth (or shrinkage) rate of a given size in the distribution. These experimental values of dx_i/dt were compared to calculated values obtained from Equations 3 and 4. The present study differed from the former (7) in that a) a series of D (Equation 3) and K_1 (Equation 4) values were used in order to find the value that best fit the data for each of the two models, and b) the difference in time over which the experimental dx_i/dt values were determined was subdivided into about 100 time increments for the evaluation of dx_i/dt values from Equations 3 and 4. This second change from the former method of analysis provided a more continuous variation in the size distribution over the time range between two experimentally-determined distributions. Comparison of experimental and calculated values of dx_i/dt showed that the size for zero growth rate was always larger for the experimental rates than for the rates calculated for either diffusion-controlled or interface-controlled growth (as also shown by the previous study (7)). Typical results for the Fe - 0.79C steel at 704°C in the present investigation are shown in Figure 6. The lateral displacement between the experimental and calculated growth curves is probably due to errors involved in obtaining the experimental growth curves (7) and, thus, comparison to calculated curves should be made after shifting the experimental curves in order to obtain alignment of the sizes for zero growth rate. Comparison of the curves shown in Figure 6 gives a value of K_1 (for interface-controlled growth) between 10^{-4} and 10^{-5} cm/sec or a value of D (for diffusion-controlled growth) of about 10^{-7} cm^2/sec. Selection of the appropriate rate

controlling mechanism by noting whether either K_1 or D was constant with time at the spheroidizing temperature was difficult due to inaccuracy in shifting and comparison. It should be noted though that the values of D were generally lower than those for diffusion of carbon in ferrite (11) and the values of K_1 at 704°C are in the range determined previously (7).

D. Analysis of N_T vs. t data

Equations 3 and 4 may be used to calculate the variation in the total number of particles per unit volume, N_T, as a function of time for comparison to the experimental data shown in Figure 3. This calculation was accomplished by:

i) dividing an experimental size distribution into about 20 size classes,

ii) assuming a value of D (for Equation 3) or K_1 (for Equation 4),

iii) calculating the change in size of the particles in each size class, Δx_i, for time increments, Δt, which were small compared to the time between experimental data points (about 100 increments were used),

iv) continuing step (iii), noting the times at which disappearance of the class containing the smallest particles occurred.

In those instances where this procedure reduced the number of size classes to 5, the size distribution was then reformulated into about 20 classes and the calculation was continued. The above sequence of steps provided the data necessary to calculate the change in size distribution and, thus, the change in N_T with time for any value of D or K_1.

Comparison of calculated values of N_T to the experimental values for the three steels spheroidized at three temperatures showed that the diffu-

sion-controlled growth model (Equation 3) approximated the experimental data as a function of time with only about an order of magnitude (or less) variation in D. The interface-controlled growth model (Equation 4) generally required a two to three order of magnitude variation in K_1 to fit the experimental N_T vs. t data. The results of these calculations for the Fe - 0.79C steel spheroidized at 704°C are shown in Figure 7. The size distribution at 2×10^3 sec (specimen 1A) was used to calculate the decrease in N_T with time from both Equation 3 and Equation 4 with various values of D and K_1, respectively. It can be seen in Figure 7 that the shape of the diffusion-controlled growth curve with a value of $D = 10^{-7}$ cm^2/sec most closely approximates the experimental N_T values as a function of time. In addition, calculations of N_T vs. t based on Equation 3, but starting with later experimental distributions (specimens 3A, 5A, and 6A), also indicate a good approximation of the experimental values with $10^{-8} < D < 10^{-7}$ cm^2/sec. These values are in agreement with those obtained from the dx_i/dt analysis discussed previously and show much less scatter than the D values from the dx_i/dt analysis. Figure 7 also shows that the curves of N_T vs. t calculated from Equation 4 do not conform to the shape of the experimental curves and the point-to-point fit to the data may be achieved only after several orders of magnitude variation of K_1 in Equation 4. A summary of the "best fit" values of D and K_1 at 704°C for both the Fe - 0.79C steel (Figure 7) and the Fe - 0.42C steel are presented in Table VI. The values of D for these steels have approximately the same magnitude and show much less variation with time than the values of K_1. The N_T vs. t analysis clearly defines the process to be diffusion-controlled. A summary of the "best fit" values of D using the N_T vs. t data starting with the shortest time size distribution for the three steels spheroidized at three tem-

peratures is given in Table VII.

The changes in size distribution that can be calculated from this N_T vs. t analysis give another justification for the applicability of this type of analysis to spheroidization data. Figure 8 shows the normalized size distribution curves that were calculated using the diffusion-controlled growth model (Equation 3) for the Fe - 0.79C steel at 704°C using $D = 10^{-7}$ cm^2/sec and the size distribution at $t = 2 \times 10^3$ sec (specimen 1A in Figure 7). It can be seen that the calculated distributions approach the steady-state distribution and closely approximate the normalized experimental distributions shown in Figure 5.

F. Temperature Dependence

The values of D obtained by the various methods of analysis used in the present investigation are summarized as a function of temperature in Figure 9. Values of the diffusion coefficient of carbon in ferrite, D_C (11), the diffusion coefficient of iron in ferrite, D_{Fe} (12), the coupled (volume) diffusion coefficient of Oriani, D^0 (8,9), and the coupled (composition and volume) diffusion coefficient of Li, Blakely, and Feingold, D^{LBF} (10) are shown for comparison.

It may be seen that the coupled diffusion coefficients accurately predict the temperature dependence of the D values determined by the N_T vs. t analysis. It is expected that the experimental D values should be somewhat high, since the model used (6) employs a minimum cross-sectional area of the diffusion paths between particles. Therefore, calculations using this model would result in experimental D values that were somewhat large. In addition, the experimental D values were based upon the spheroidization of the initial size distribution. Table VI and Figure 7 show that there is a tendency for the D values to decrease slightly with

time. If the effects of the cross-sectional area of the paths and the long-time D values were incorporated into Figure 9, the agreement between the experimental D values and the coupled D values would be much better.

The non-linearity of the plots of D values determined by the Lifshitz-Wagner analysis of the mean particle size shown in Figure 9 is probably due to the non-steady-state distribution exhibited by the data. It should be noted that the high-temperature data points define a slope which approached that of the coupled D values and that of the N_T vs. t data. However, the departure from the steady-state condition at lower temperatures brings about considerable error in using this analysis. It is conceivable that this is the reason that Ranovh, Modin and Modin (5) found that the Lifshitz-Wagner analysis was not applicable to their data obtained at temperatures below 700°C.

IV. SUMMARY AND CONCLUSIONS

The present investigation provides spheroidization data for cementite in iron-carbon alloys over ranges of carbon content, temperature, and time. Because of the purity of the binary alloys that were studied, the results obtained could be compared to the various existing spheroidization models for binary alloys. It may be concluded from this comparison that:

1. The experimentally-determined size distributions of cementite particles approach the Lifshitz-Wagner steady-state distribution, but do not reach it in times up to about 10^6 sec.
2. The $\bar{R}$ vs. t analysis of spheroidization (Lifshitz-Wagner) may lead to errors in data analysis if the departure from the steady-state size distribution is large. The departures from the steady-state size distribution are smallest at the highest spheroidizing

temperatures and, thus, the errors in using the Lifshitz-Wagner treatment are lowest in this range of temperature.

3. The mathematical model proposed previously (6) provides a means for analyzing spheroidization data for size distributions which are not at steady-state.

4. Analysis of N_T vs. t data provides similar results with much less data scatter than the method of analysis of growth (and shrinkage) rates of individual size classes (dx_i/dt) (7).

5. The analysis of N_T vs. t data in terms of previously-developed models (6) indicates that the spheroidization of binary iron-carbon alloys is controlled by long-range diffusion. The appropriate diffusion coefficient lies between the extremes of the diffusion coefficients of iron and carbon in ferrite. A coupled diffusion coefficient, of the types proposed by Oriani (8,9) and Li, Blakely, and Feingold (10), appears to be applicable.

V. ACKNOWLEDGMENTS

The authors gratefully acknowledge the support of this research by the Office of Naval Research under ONR Contract No. N0014-67-A-0406-0002. The authors also express their appreciation to the U.S. Steel Corporation, Fundamental Research Laboratory, for supplying the steels used in the present investigation and to Mr. Richard Zaehring who assisted in the quantitative metallography.

REFERENCES

1. C. Wagner: Z. Electrochem., 1961, vol. 65, p. 581.
2. I. M. Lifshitz and V. V. Slyozov: Zh. Eksperim. i Teor. Fiz., 1958, vol. 35, p. 479.
3. I. M. Lifshitz and V. V. Slyozov: Fiz. Tverd. Tela, 1959, vol. 1, p. 1401.
4. I. M. Lifshitz and V. V. Slyozov: Phys. Chem. Solids, 1961, vol. 19, p. 35.
5. O. Bannyh, H. Modin, and S. Modin: Jernkontorets Ann., 1962, vol. 146, p. 744.
6. R. W. Heckel: Trans. Met. Soc. AIME, 1965, vol. 233, p. 1994.
7. R. W. Heckel and R. L. DeGregorio: Trans. Met. Soc. AIME, 1965, vol. 233, p. 2001.
8. R. A. Oriani: Acta Met., 1964, vol. 12, p. 1399.
9. R. A. Oriani: Acta Met., 1966, vol. 814, p. 84.
10. Che-Yu Li, J. M. Blakely, and A. H. Feingold: Acta Met., 1966, vol. 14, p. 1397.
11. P. P. Smith: Trans. Met. Soc. AIME, 1962, vol. 224, p. 195.
12. R. J. Borg and D. Y. F. Lai: Acta Met., 1963, vol. 11, p. 861.
    F. S. Buffington, K. Hirano and M. Cohen: Acta Met., 1961, vol. 9, p. 434.
13. G. P. Airey, T. A. Hughes, and R. F. Mehl: Trans. Met. Soc. AIME, 1968, vol. 242, p. 1353.
14. R. T. DeHoff: Trans. Met. Soc. AIME, 1962, vol. 224, p. 774.
15. C. S. Smith and L. Guttman: Trans. AIME, 1953, vol. 197, p. 81.
16. A. J. Ardell and R. B. Nicholson: J. Phys. Chem. Solids, 1966, vol. 27, p. 1793.
17. C. A. Wert: Trans. AIME, 1950, vol. 188, p. 1242.

Table I

Composition of steels (weight percent) used in the present investigation

	C*	Cr	Ni	Si	Co	Cu	V	Mo
Fe-0.24C	0.24	N.F.	N.F.	0.00X	0.00X	0.00X	0.00X	0.00X
Fe-0.42C	0.42	0.002**	0.075**	0.00X	0.00X	0.00X	0.00X	0.00X
Fe-0.79C	0.79	0.004**	N.F.	0.022**	0.00X	0.00X	0.00X	0.00X

*combustion
**wet chemistry

all other elements analyzed by spectrographic analysis
N.F. - not found by spectrographic analysis

Table II

Summary of austenitizing and spheroidizing heat treatment* conditions used in the present investigation

	Austenitizing treatment+ Temperature	Time	Range of spheroidizing times (sec) at different temperatures		
	(°C)	(min)	704°C	649°C	594°C
Fe - 0.24C	855	8	2×10^3 to 1×10^6	7×10^3 to 3×10^5	2×10^4 to 1×10^6
Fe - 0.42C	815	8			
Fe - 0.79C	755	8			

* All heat treatments carried out in salt baths
\+ Austenitizing followed by water quench

Table III

Values of the axial ratio of oblate ellipsoids of revolution, q, as a function of steel composition and spheroidizing conditions

Time (sec) of spheroidizing at 704°C

	2×10^3	7×10^3	20×10^3	50×10^3	100×10^3	200×10^3	350×10^3	1000×10^3
Fe - 0.24C	0.55	0.75			0.85			1.00
Fe - 0.42C	0.60		0.55	0.90	0.70	0.75		1.00
Fe - 0.79C	0.65	0.75	0.75	0.75	0.75	0.95	0.80	0.65

Time (sec) of spheroidizing at 649°C

	7×10^3	20×10^3	100×10^3	300×10^3
Fe - 0.24C	0.60	0.60	0.70	0.75
Fe - 0.42C	0.60	0.55	0.70	0.70
Fe - 0.79C	0.70	0.75	0.95	0.55

Time (sec) of spheroidizing at 594°C

	20×10^3	100×10^3	200×10^3	350×10^3	500×10^3	1000×10^3
Fe - 0.24C	0.80	0.60		0.65	0.55	0.60
Fe - 0.42C	0.90	0.70	0.75	0.90		0.60
Fe - 0.79C	0.90	0.75	0.80	0.65	0.60	0.70

Table IV

Slopes for plots of $\log(\bar{k} - \bar{R}_o^3)$ vs. $\log(t - t_o)$

(from Figure 4)

	Temperature (C°)		
	704	659	594
Fe - 0.24C	0.74	0.79	0.86
Fe - 0.42C	0.72	0.68	0.58
Fe - 0.79C	1.02	0.85	0.70

Table V

Values of D (cm^2/sec) obtained from $\bar{R}$ vs. t analysis

	Temperature (C°)		
	704	649	594
Fe - 0.24C	1.4×10^{-8}	1.8×10^{-9}	1.2×10^{-9}
Fe - 0.42C	1.8×10^{-8}	3.3×10^{-9}	1.5×10^{-9}
Fe - 0.79C	6.0×10^{-8}	6.0×10^{-9}	3.0×10^{-9}

Table VI

Summary of values of D (cm^2/sec) and K_1 (cm/sec) which provide the best fit to the N_T vs. t data for the Fe - 0.42C and Fe - 0.79C steels spheroidized at 704°C. Values are listed according to the spheroidizing time of the specimen used to obtain the experimentally-determined size distribution which was used as the starting point for the calculation using Equation 3 and Equation 4.

Values of D and K_1 to get best fit of N_T vs. t starting with experimental size distribution obtained at 704°C after the following times (sec):

		2×10^3	20×10^3	100×10^3	200×10^3
Fe - 0.42C	D	9×10^{-8}	2×10^{-8}	1×10^{-8}	1×10^{-8}
Fe - 0.42C	K_1	400×10^{-6}	20×10^{-6}	3×10^{-6}	0.7×10^{-6}
Fe - 0.79C	D	10×10^{-8}	5×10^{-8}	3×10^{-8}	1×10^{-8}
Fe - 0.79C	K_1	600×10^{-6}	100×10^{-6}	10×10^{-6}	1×10^{-6}

Table VII

Summary of values of D which provide the best fit of Equation 3 to the N_T vs. t data for the three steels and three spheroidizing temperatures studied. The experimentally-determined size distribution used with Equation 3 was obtained from specimens spheroidized for the shortest length of time (see Table III) in order to provide a fit over the widest possible time range.

	Temperature (°C)	D (cm^2/sec)
Fe - 0.24C	704	1.5×10^{-7}
Fe - 0.42C	704	9×10^{-8}
Fe - 0.79C	704	1×10^{-7}
Fe - 0.24C	649	1.4×10^{-8}
Fe - 0.42C	649	1.2×10^{-8}
Fe - 0.79C	649	1×10^{-8}
Fe - 0.24C	594	1.4×10^{-9}
Fe - 0.42C	594	1.2×10^{-9}
Fe - 0.79C	594	1.1×10^{-9}

Figure Captions

Figure 1 - Photomicrographs showing the change in size distributions of cementite in ferrite in the Fe - 0.79C steel as a function of time of spheroidizing at 704°C. X750
(a) specimen 1A (2×10^3 sec); (b) specimen 3A (2×10^4 sec);
(c) specimen 6A (2×10^5 sec); (d) specimen 9A (1×10^6 sec).

Figure 2 - Number of particles per unit volume, N_j, in a given size class as a function of its mean particle size, R_j, for the Fe - 0.79C steel spheroidized at 704°C.

Figure 3 - Total number of particles per unit volume, N_T, as a function of spheroidizing time, t, for the three steels and three temperatures studied in the present investigation.

Figure 4 - Variation of the mean particle radius, $\bar{R}$, with spheroidizing time, t, plotted in the form of $(\bar{R}^3 - \bar{R}_o^3)$ as a function of $(t - t_o)$ for the three steels and three temperatures studied in the present investigation. $\bar{R}_o$ and t_o values are taken from the shortest spheroidizing times studied.

Figure 5 - Normalized size distribution curves for the experimental data for the Fe - 0.79C steel spheroidized at 704°C, compared with each other and with the steady-state size distribution predicted by the Lifshitz-Wagner theory.

Figure 6 - The experimental rates of growth of particles in a given size class, dx_i/dt, are plotted as a function of the size of particles in the size class, x_i, for particles in specimen 1A growing to particles in specimen 2A (Fe - 0.79C steel spheroidized at 704°C). These are compared with the calculated rates based on the diffusion-controlled and the interface-controlled growth models.

Figure 7 - The experimental variation of the total number of particles, N_T, as a function of spheroidizing time, t, compared with the calculated variations. The calculated variations are based on the diffusion-controlled and the interface-controlled growth models. Variations are calculated from different starting size distributions for the Fe - 0.79C steel spheroidized at 704°C.

Figure 8 - Normalized size distribution curves, calculated for the Fe - 0.79C steel spheroidized at 704°C, using the diffusion-controlled growth model, compared to the steady-state size distribution curve predicted by the Lifshitz-Wagner theory. The value of $D = 10^{-7}$ cm^2/sec and specimen 1A as the starting size distribution were used for the calculation.

Figure 9 - Plots of diffusion coefficient, D, as a function of inverse temperature, $1/T$. D_C and D_{Fe} were obtained from literature (11,12). D^0 and D^{LBF} were calculated using Equations 6 and 7. Values obtained from the N_T and $\bar{R}$ analyses are compared to these values.

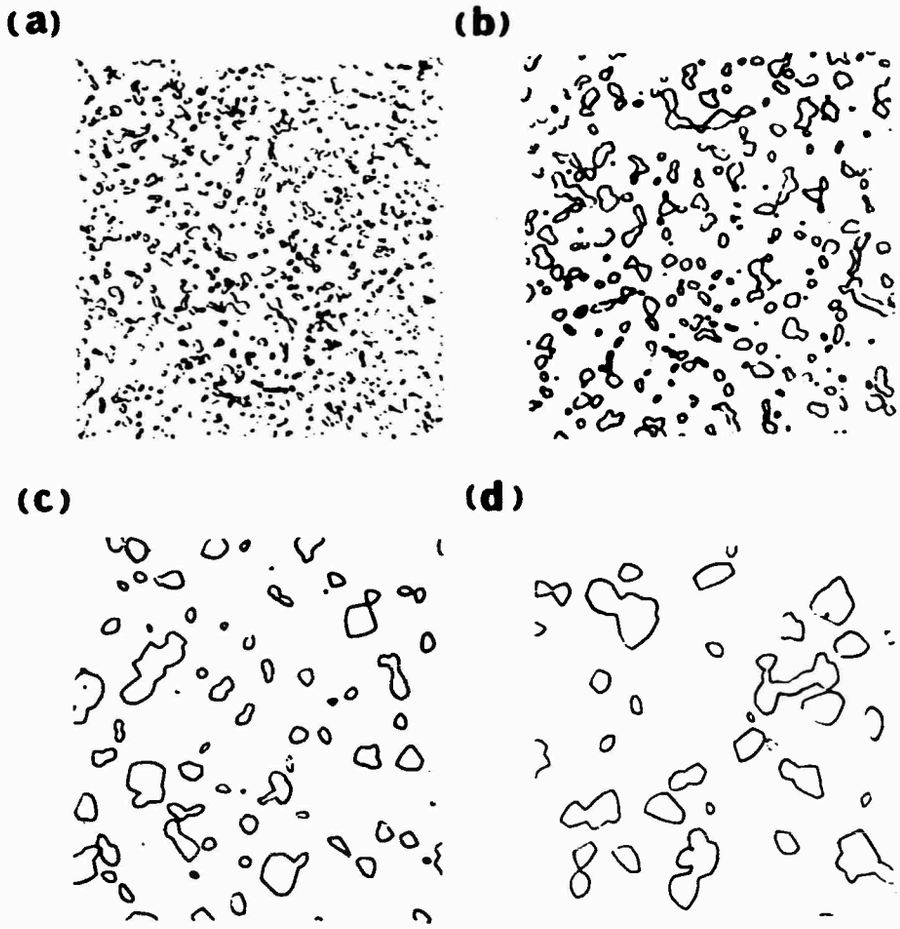

Figure 1 - Photomicrographs showing the change in size distribution of cementite in ferrite in the Fe - 0.79C steel as a function of time of spheroidizing at 704°C. X750

(a) specimen 1A (2×10^3 sec); (b) specimen 3A (2×10^4 sec);
(c) specimen 6A (2×10^5 sec); (d) specimen 9A (1×10^6 sec).

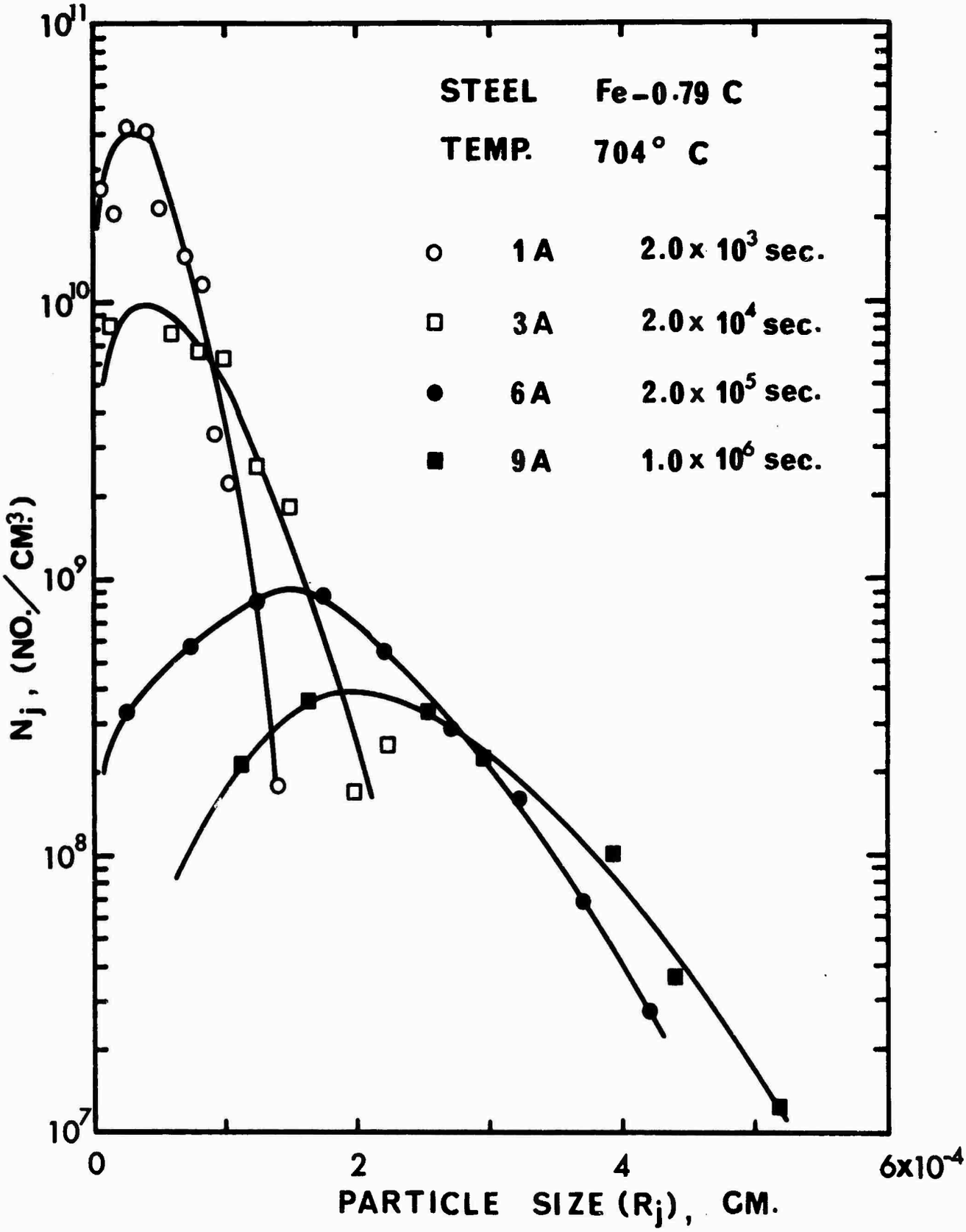

Figure 2 - Number of particles per unit volume, N_j, in a given size class as a function of its mean particle size, R_j, for the Fe - 0.79C steel spheroidized at 704°C.

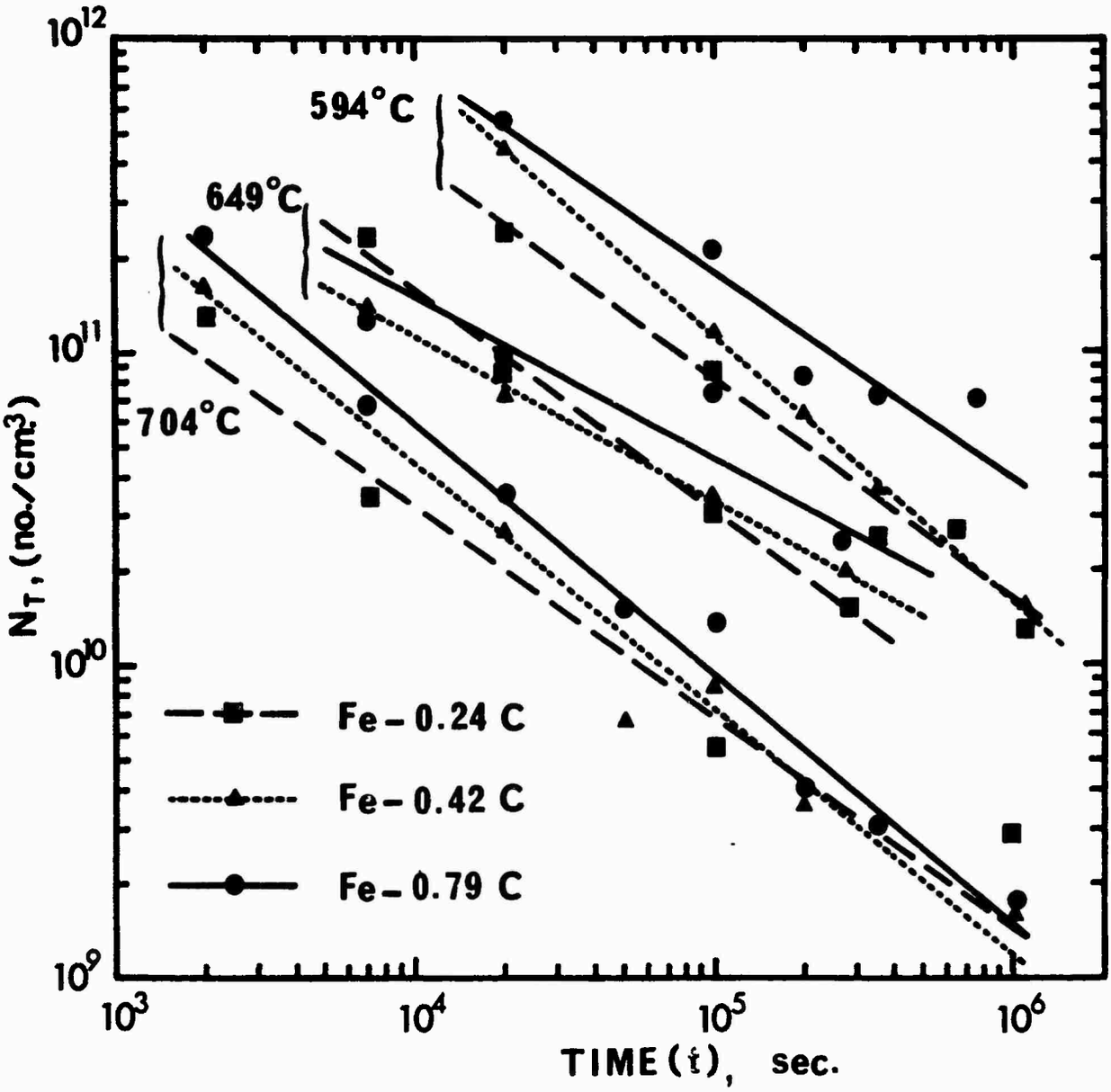

Figure 3 - Total number of particles per unit volume, N_T, as a function of spheroidizing time, t, for the three steels and three temperatures studied in the present investigation.

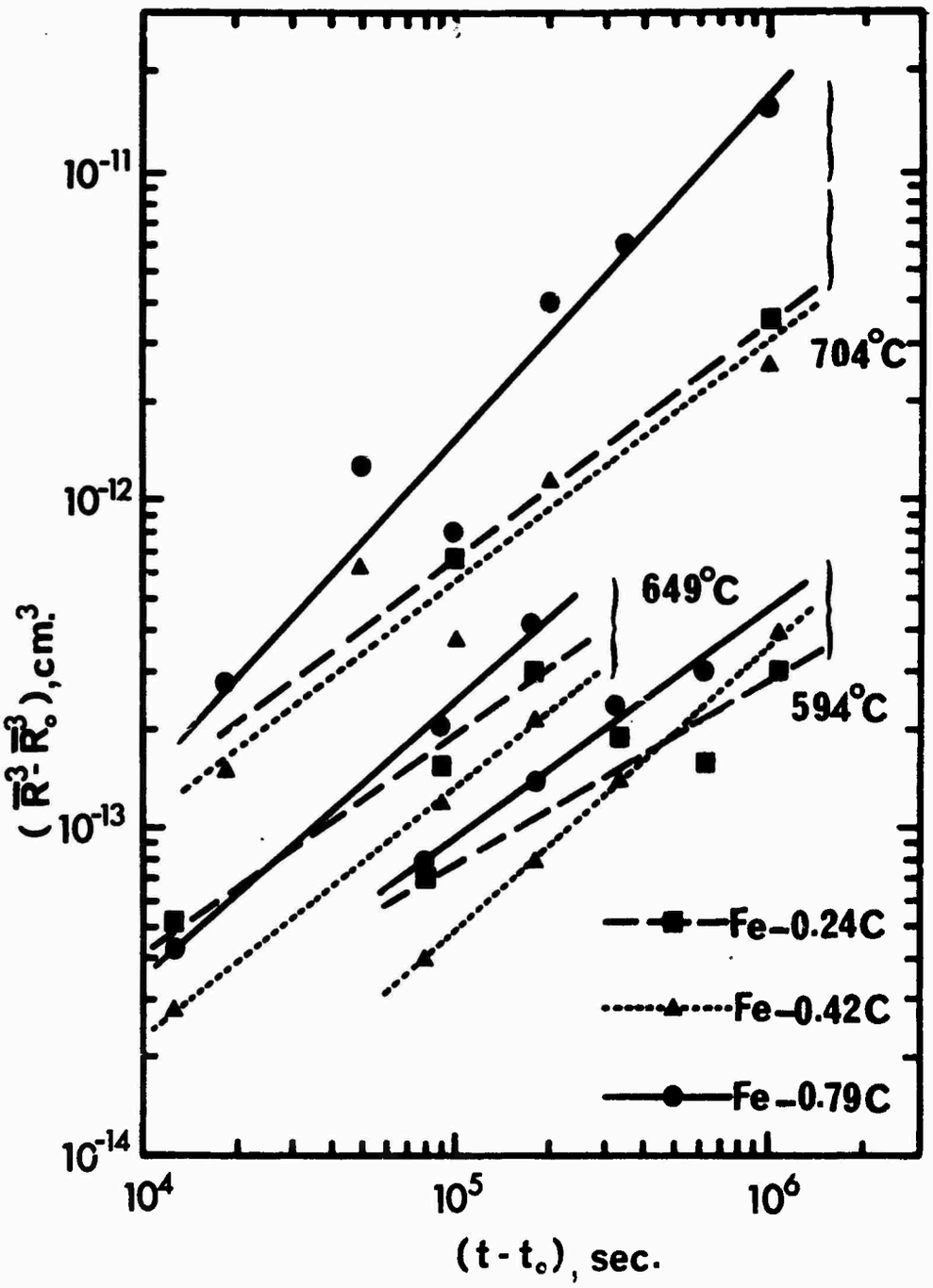

Figure 4 - Variation of the mean particle radius, $\bar{R}$, with a spheroidizing time, t, plotted in the form of ($\bar{R}^3 - \bar{R}_o^3$) as a function of $(t - t_o)$ for the three steels and three temperatures studied in the present investigation. $\bar{R}_o$ and t_o values are taken from the shortest spheroidizing times studied.

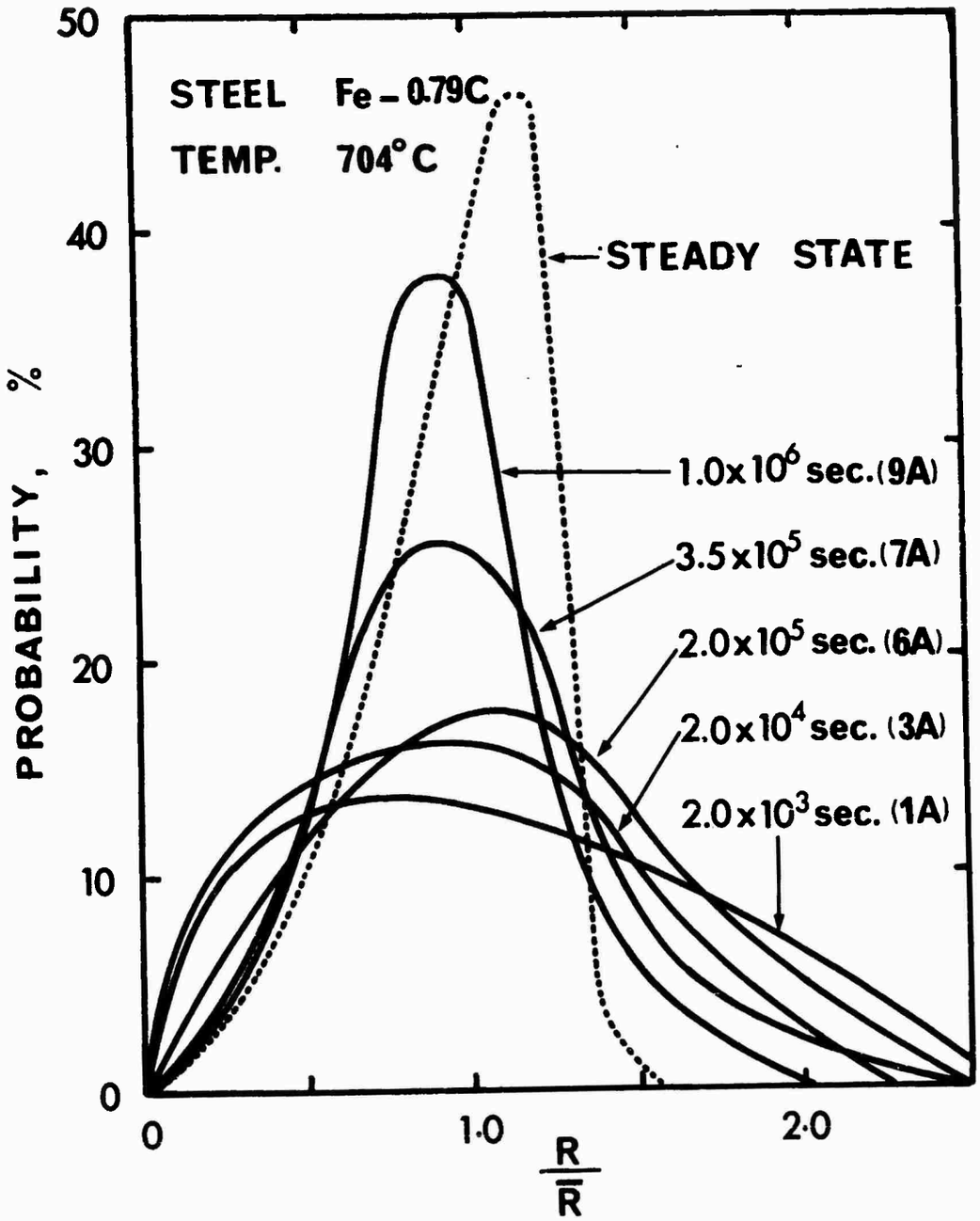

Figure 5 - Normalized size distribution curves for the experimental data for the Fe - 0.79C steel spheroidized at 704°C, compared with each other and with the steady-state size distribution predicted by the Lifshitz-Wagner theory.

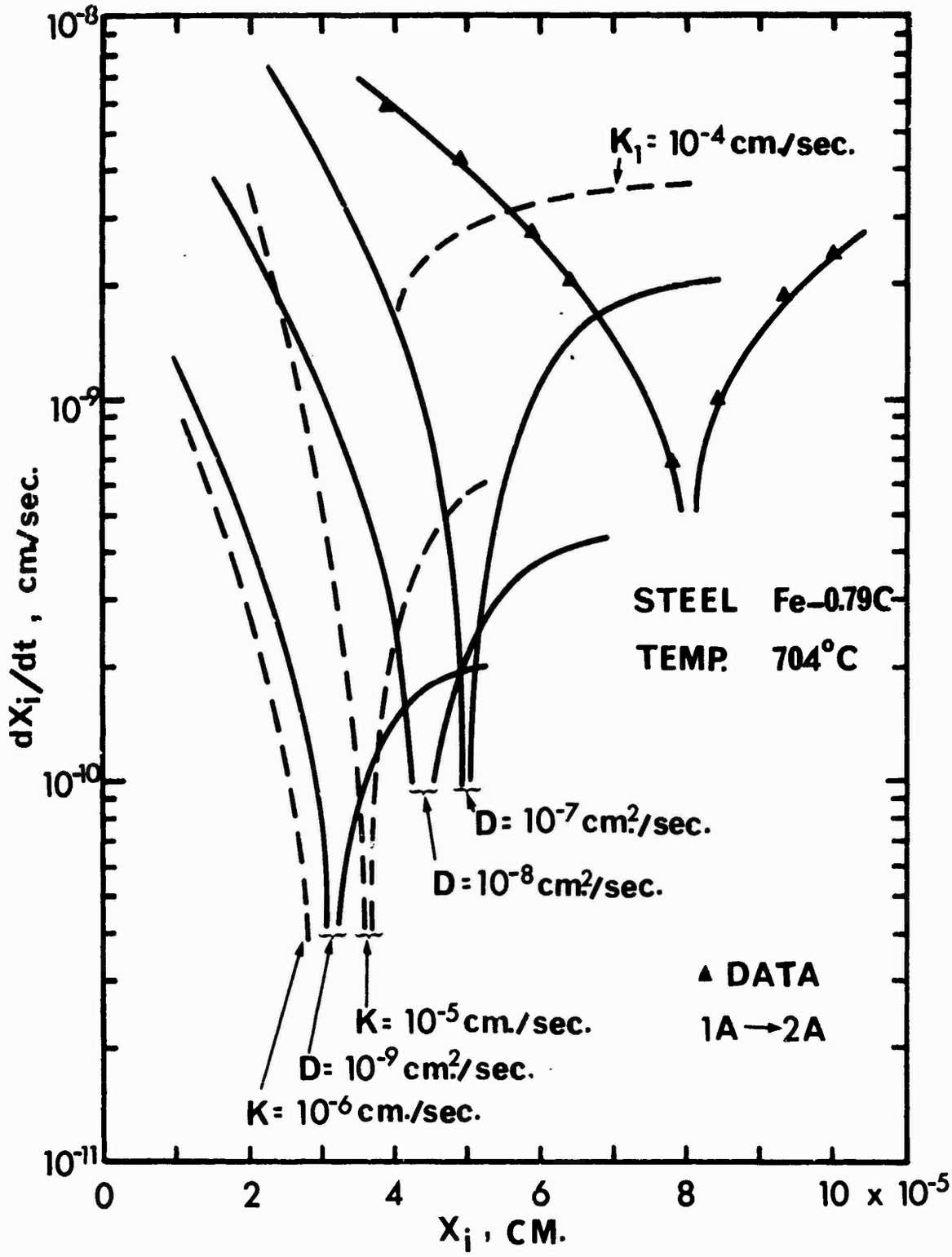

Figure 6 - The experimental rates of growth of particles in a given size class, dx_i/dt , are plotted as a function of the size of particles in the size class, x_i , for particles in specimen 1A growing to particles in specimen 2A (Fe - 0.79C steel spheroidized at 704°C). These are compared with the calculated rates based on the diffusion-controlled and the interface-controlled growth models.

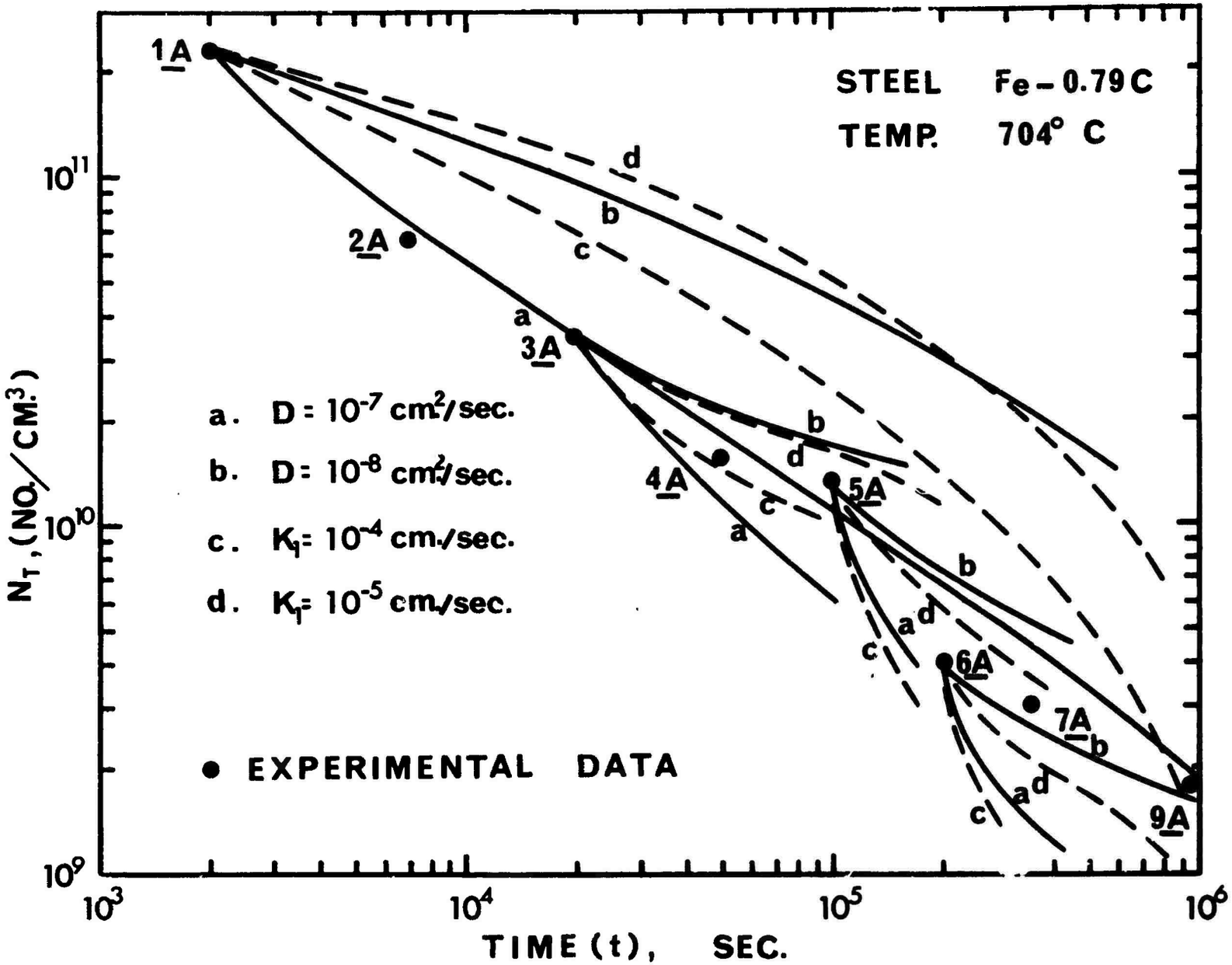

Figure 7 - The experimental variation of the total number of particles, N_T, as a function of spheroidizing time, t, compared with the calculated variations. The calculated variations are based on the diffusion-controlled and the interface-controlled growth models. Variations are calculated from the different starting size distributions for the Fe - 0.79C steel spheroidized at 704°C.

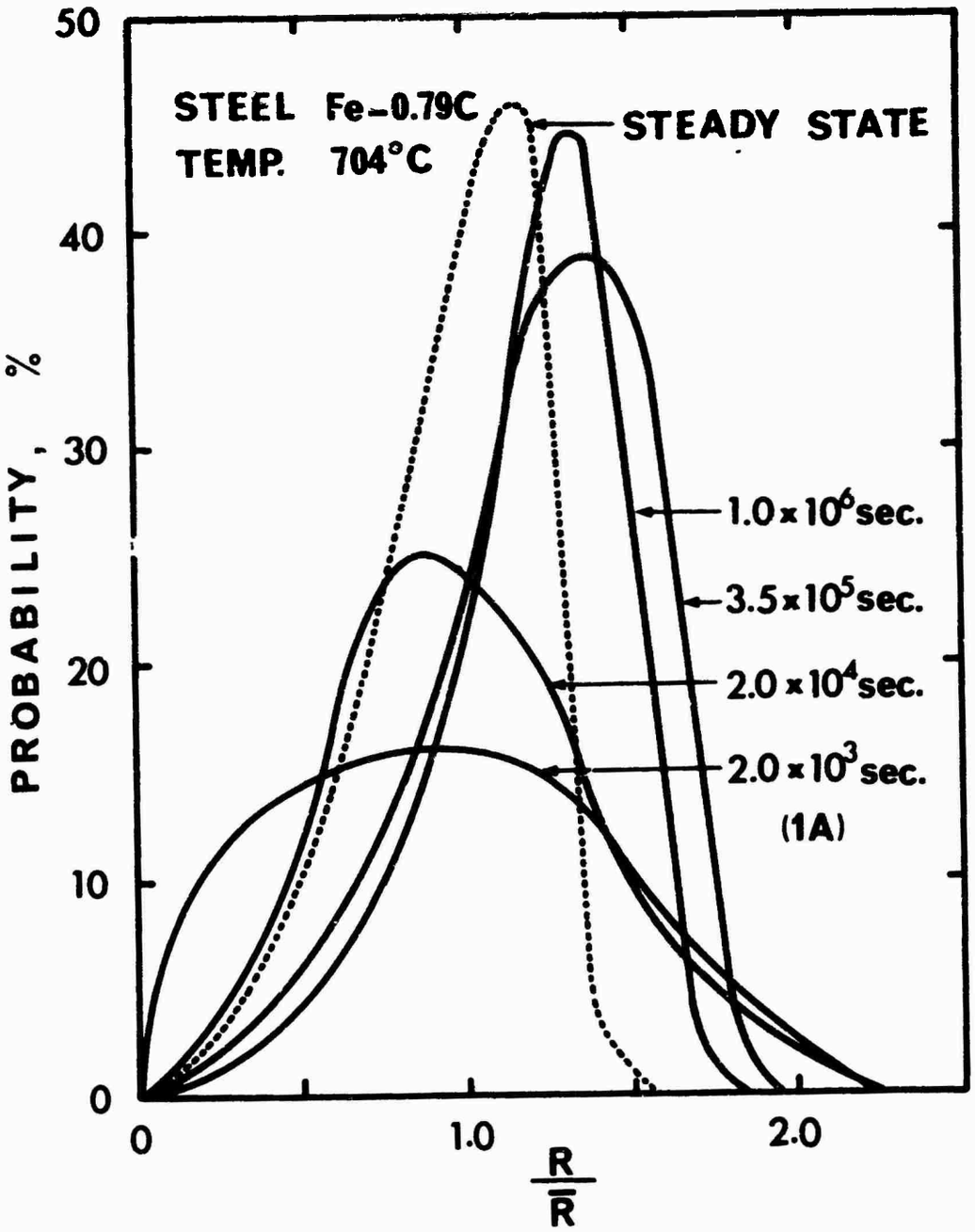

Figure 8 - Normalized size distribution curves, calculated for the Fe - 0.79C steel spheroidized at 704°C, using the diffusion-controlled growth model, compared to the steady-state size distribution curve predicted by the Lifshitz-Wagner theory. The value of $D = 10^{-7}$ cm^2/sec and specimen 1A as the starting size distribution were used for the calculation.

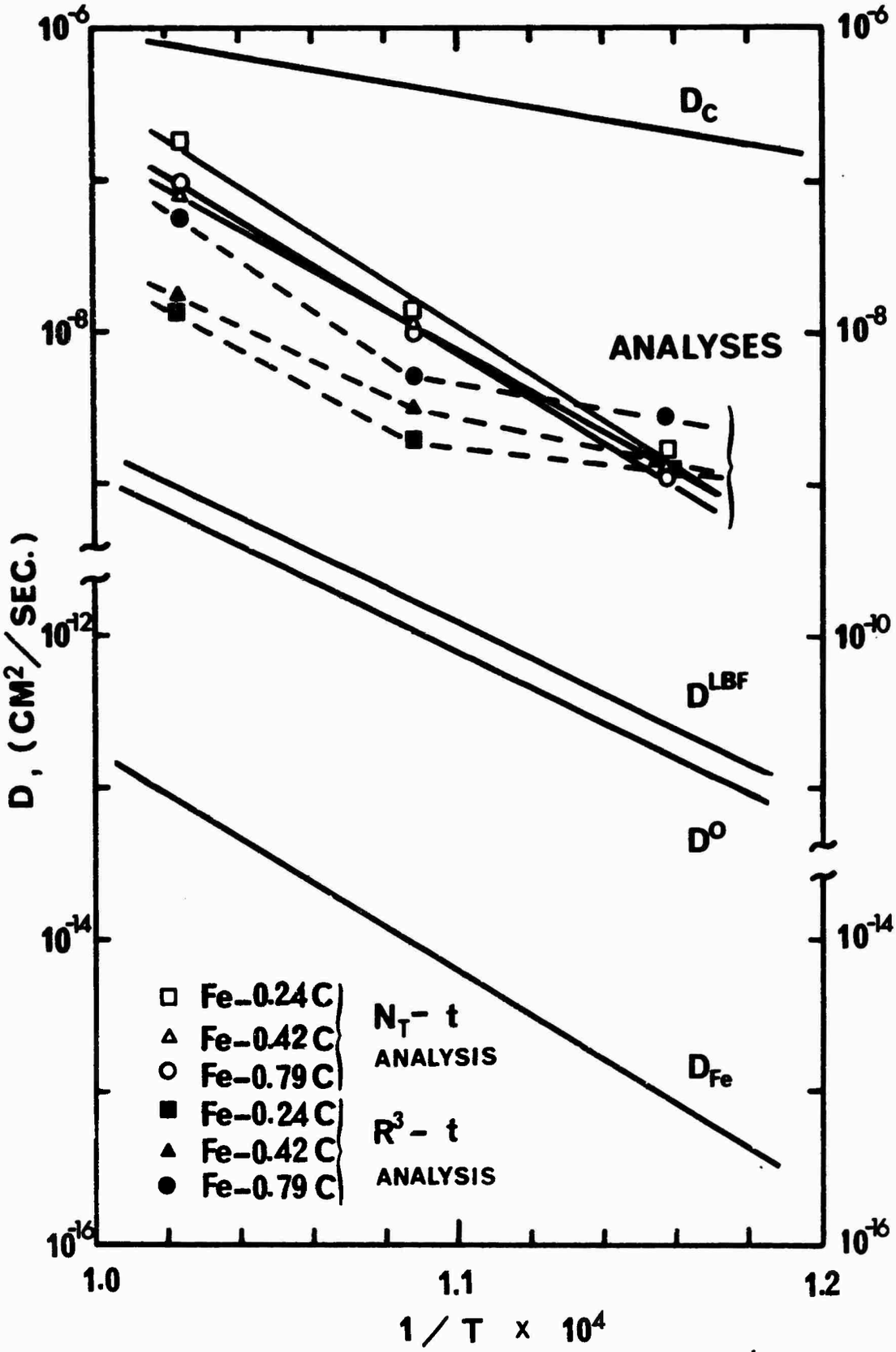

Figure 9 - Plots of diffusion coefficient, D, as a function of inverse temperature, $1/T$. D_c and D_{Fe} were obtained from literature (11, 12) D^o and D^{LBF} were calculated using Equations 6 and 7. Values obtained from the N_T and $\bar{R}$ analyses are compared to these values.

Unclassified
Security Classification

AD 707798

DOCUMENT CONTROL DATA - R & D

(Security classification of title, body of abstract and indexing annotation must be entered when the overall report is classified)

1. ORIGINATING ACTIVITY (Corporate author) Drexel Institute of Technology Department of Metallurgical Engineering Philadelphia, Pa. 19104	2a. REPORT SECURITY CLASSIFICATION Unclassified 2b. GROUP

3. REPORT TITLE

"SPHEROIDIZATION OF BINARY IRON-CARBON ALLOYS OVER A RANGE OF TEMPERATURES"

4. DESCRIPTIVE NOTES (Type of report and inclusive dates)

Technical Report No. 1

5. AUTHOR(S) (First name, middle initial, last name)

Richard W. Heckel
Krishna M. Vedula

6. REPORT DATE April 1969	7a. TOTAL NO. OF PAGES 45	7b. NO. OF REFS 17

8a. CONTRACT OR GRANT NO N00014-67-A-0406-0002 b. PROJECT NO d.	9a. ORIGINATOR'S REPORT NUMBER(S) Research Project 337 Technical Report No. 1 9b. OTHER REPORT NO(S) (Any other numbers that may be assigned this report)

10. DISTRIBUTION STATEMENT

Reproduction in whole or in part is permitted for any purpose of the United States Government. Distribution of this document is unlimited.

11. SUPPLEMENTARY NOTES	12. SPONSORING MILITARY ACTIVITY Metallurgy Branch Office of Naval Research Washington, D. C. 20360

13. ABSTRACT

The spheroidization of cementite in binary iron-carbon alloys (0.24, 0.42, and 0.79 weight percent carbon) was investigated over a range of temperatures (594, 649, and 704°C) for times up to about 10^6 seconds. Quantitative metallography techniques were used to obtain the following microstructural data on the cementite particles: shape, size distribution, mean size, number of particles per unit volume, and growth (and shrinkage) rates of various sizes in the size distribution. The variations of these microstructural parameters were analyzed in terms of existing models for the spheroidization process.

The Lifshitz-Wagner analysis is shown to have limited applicability to the spheroidization of cementite in binary steels, since the required steady-state size distribution is not attained in times less than about 10^6 seconds. An analysis similar to that of Lifshitz and Wagner, but requiring no specification of the shape of the size distribution, is shown to apply and indicates that the observed spheroidization was diffusion-controlled. The effective diffusion coefficient was between the values for the diffusion of carbon and iron in ferrite and approximated the coupled diffusion coefficients developed by Oriani and Li, Blakely, and Feingold.

DD FORM 1 NOV 65 1473

Security Classification

Unclassified

Security Classification

14 KEY WORDS	LINK A ROLE	LINK A WT	LINK B ROLE	LINK B WT	LINK C ROLE	LINK C WT
Iron-carbon alloys						
Spheroidization						
Coarsening						
Ostwald ripening						
Quantitative metallography						

Security Classification